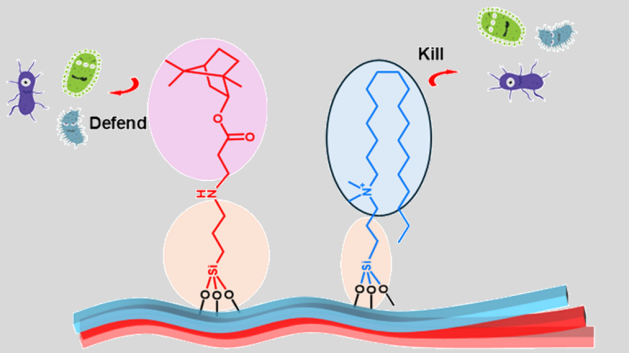
Research Article

Organosilicon Borneol Ester/Quaternary Ammonium Salt Based Attack-Defense Coatings for Durable Antibacterial and Antifungal Cotton Textiles

NIU Wenjing, WANG Songtao, LIU Yi, LIANG Wanli, XIE Wensheng, LI Guofeng and WANG Xing✉

Received May 30, 2026
Accepted July 1, 2026
© Jilin University, The Editorial Department of Chemical Research in Chinese Universities and Springer-Verlag GmbH

Cotton textiles (CTs) are in high demand for antimicrobial applications. Traditional approaches often struggle to achieve antibacterial and antifungal efficacy simultaneously. Herein, organosilicon quaternary ammonium salt (QAS/AEM-5700, a contact bactericidal agent) and organosilicon borneol ester (SBA, a stereochemical anti-adhesive agent) are covalently co-grafted onto CT surfaces *via* siloxane hydrolytic condensation, generating a synergistic antimicrobial coating (CT-A/S) that integrates both offensive and defensive functionalities. The as-prepared CT-A/S exhibits excellent antimicrobial activity against *Escherichia coli* (*E. coli*), *Staphylococcus aureus* (*S. aureus*), and *Aspergillus niger* (*A. niger*), with antimicrobial rates approaching 100%. Owing to the covalent immobilization, the CT-A/S demonstrates outstanding laundering durability. This strategy not only overcomes the deficiency of QAS-modified CT in mold resistance, but also addresses the limitation of borneol ester in contact-based bacterial killing. Furthermore, an *in vivo* mice infection model validates the antibacterial and anti-infective efficacy of the coating, offering a promising approach for the long-term antimicrobial protection of healthcare textiles.



Keywords Quaternary ammonium salt; Organosilicon borneol ester; Cotton textile; Antimicrobial coating; Synergistic effect

1 Introduction

The adhesion, colonization, and proliferation of microorganisms on textile surfaces represent significant contributors to the cross-transmission of hospital-acquired infections, hygiene risks associated with public health products, and constraints on the practical application of functional textiles.[1] As materials that undergo prolonged and intimate contact with human skin, textiles by virtue of their fibrous architecture and inherent moisture-retention characteristics provide an optimal micro-environment for the growth of bacteria and fungi.[2] Statistical evidence indicates that approximately 1.7 million hospital-acquired infections occur annually in U.S. healthcare facilities, with healthcare workers' uniforms frequently serving as contaminated fomites during routine clinical practice and acting as critical vectors for pathogen transmission to both patients and the broader healthcare environment.[3,4] Consequently, the development of antimicrobial textiles exhibiting high efficacy, broad-spectrum activity, long-term durability, and environmental compatibility has garnered substantial research interest.[5,6]

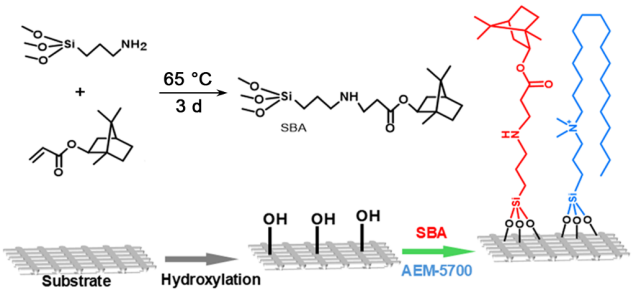
Quaternary ammonium salts (QASs) have been extensively investigated and commercially deployed in textile finishing applications, attributable to their broad-spectrum bactericidal efficacy, favorable chemical stability, and cost-effectiveness.[7,8] The antimicrobial mechanism of QASs is predicated upon electrostatic interactions between their cationic head groups and the negatively charged bacterial cell envelope, which disrupt membrane integrity, induce intracellular component leakage, and ultimately precipitate cell death.[9] This contact-killing modality confers rapid bactericidal action upon QASs and is associated with a comparatively low propensity for inducing bacterial resistance.[10] Nevertheless, conventional QASs are typically incorporated into textiles through physical adsorption or pad-dry-cure processes, resulting in weak non-covalent interactions with the fiber matrix. The antimicrobial moieties are susceptible to leaching during repeated laundering and

✉ WANG Xing
wangxing@mail.buct.edu.cn
State Key Laboratory of Organic-Inorganic Composites, Beijing Laboratory of Biomedical Materials, College of Life Science and Technology, Beijing University of Chemical Technology, Beijing 100029, P. R. China

prolonged usage, thereby compromising antimicrobial durability.[11,12] A representative example is AEM-5700, an organosilicon QAS, which has been widely employed as an antimicrobial agent.[13] Notably, the cationic antimicrobial materials render it challenging to achieve the desired dual functionality of antimicrobial efficacy coupled with antifouling properties in practical applications, as the accumulation of dead bacterial residues on material surfaces can progressively diminish long-term antimicrobial performance. The conceptualization of functional materials integrating both bactericidal and anti-adhesive mechanisms has accordingly emerged as a prominent research frontier.

Natural borneol, a terpenoid natural product distinguished by its chiral stereostructure, has demonstrated considerable potential in antimicrobial material design in recent years.[14−16] Beyond its intrinsic antibacterial activity, borneol is capable of modulating microbial behavior at material interfaces through stereochemical recognition mechanisms, microorganisms actively detach from surfaces upon encountering these stereochemical motifs, thereby imparting antimicrobial adhesion resistance.[17,18] This distinctive passive defense mechanism is mechanistically complementary to the active attack bactericidal mode of QASs, presenting an opportunity to construct an integrated offensive and defensive antimicrobial functional system.[19−22] Prior work shows alkyl QAS conjugated with *L*-bornyl ester displays dual bactericidal and anti-adhesive activity in solution and degrades into borneol under weak alkaline conditions.[23] Still, their synergistic effect only works in liquid systems. Current cotton finishing methods immobilize only one functional component, namely QAS for contact-killing or borneol derivatives for anti-adhesion. Few approaches can covalently co-anchor organosilicon QAS and organosilicon bornyl ester on cellulose fibers to construct dual-functional coatings, which limits the production of cotton fabrics with integrated broad-spectrum antibacterial, antifungal and wash-resistant properties.

In this study, we report a covalent co-grafting strategy for the fabrication of a synergistic antimicrobial coating on cotton textiles (CTs), utilizing organosilicon QAS (AEM-5700) and organosilicon borneol ester (SBA) as dual functional units. The SBA precursor was synthesized *via* an aza-Michael addition reaction between isobornyl acrylate (IBO) and (3-aminopropyl)-trimethoxysilane (APTMS). Subsequently, SBA and AEM-5700 were co-immobilized onto CT surfaces through siloxane hydrolysis and thermal curing (Scheme 1). Through optimization of the grafting process parameters, both active components were covalently anchored to the cellulose substrate *via* silanol condensation, ensuring robust and durable surface attachment. The passive defense (anti-adhesion) conferred by the borneol structural motif and



Scheme 1 Synthesis process and antibacterial mechanism of modified materials

the active attack (contact bactericidal action) of the long-chain QAS operate in concert to surmount the intrinsic limitations of single-mechanism antimicrobial strategies. A comprehensive evaluation of the antimicrobial performance, bacterial adhesion resistance, and laundering durability of the modified textiles was conducted, yielding a class of long-lasting and stable antimicrobial materials. Furthermore, medical gauze was identified as a particularly suitable candidate for this modification strategy, underscoring the translational potential of this approach for clinical textile applications.

2 Results and Discussion

2.1 Characterization

2.1.1 Surface and Composition Characterization

A co-synthesis strategy was employed for the covalent grafting and functionalization of different substrates. First, a hydroxyl-rich material was selected as the representative of hydroxyl-rich substrates and underwent direct surface modification. SBA was synthesized *via* a solvent-free aza-Michael addition reaction between APTMS and IBO. Subsequently, CT-S was obtained *via* a covalent method by grafting SBA onto the surface groups of CT through silane hydrolysis. Next, AEM-5700 and a mixture of SBA and AEM-5700 were grafted onto the material surface *via* silane hydrolysis, yielding CT-A and CT-A/S, respectively. Fig. 1A shows optical photographs of the CT fabric before and after modification. Compared to the white CT, CT-S, CT-A, and CT-A/S exhibit a yellowish tint due to the introduction of SBA and AEM-5700. Additionally, energy dispentive X-ray spectroscopy (EDS) analysis was employed to evaluate the uniformity of the surface modification. As shown in Fig. 1B, the introduced elements Si and Cl are uniformly distributed across the fiber surface, indicating that the modification is relatively uniform.

The surface modification of CT was confirmed *via* water contact angle (WCA) measurements. As shown in Fig. 1C, the contact angle of CT decreased from 122.3°±5° to 0°;

https://doi.org/10.1007/s40242-026-6123-z

following covalent grafting with SBA, the contact angle remained unchanged, indicating enhanced surface hydrophobicity. The pristine unmodified CT exhibited a high water contact angle of 122.3°±5°, which was attributed to residual sizing and hydrophobic finishing agents introduced during industrial textile production. These surface additives shielded cellulose hydroxyl groups and endowed the fabric with hydrophobicity. After complete pretreatment to remove all residual finishing chemicals, bare cellulose fibers with abundant exposed —OH were obtained for subsequent silane co-grafting. In contrast, after covalent grafting with AEM-5700, the contact angle changed more significantly, with enhanced hydrophilicity. When both SBA and AEM-5700 were covalently grafted, the CT surface exhibited pronounced hydrophobicity.

2.1.2 Characterization by Fourier-transform Infrared Spectroscopy

Fourier-transform infrared spectroscopy (FTIR) analysis was used to further investigate changes in chemical bonds before and after material modification (Fig. 2A). Both the pre- and post-modified CT fabrics exhibited characteristic peaks at 3277, 2950, 2895, and 1027 cm^{-1}, which are attributed to the stretching vibrations of —OH, —CH_3, —CH_2, and C—O. The absorption peak at 800 cm^{-1} is attributed to Si—C stretching vibrations. Compared to CT, CT-S, CT-A, and CT-A/S exhibit C—N (1551, 1550, and 1550 cm^{-1}). Furthermore, compared to CT-A, CT-A and CT-A/S contain ester bonds in their surface structures. Consequently, new C═O—C absorption peaks are observed at 1730 and 1726 cm^{-1}, respectively. The FTIR results provide solid evidence of the success of the surface modification.

2.1.3 X-Ray Photoelectron Spectroscopy Characterization

The key chemical bond energies of the

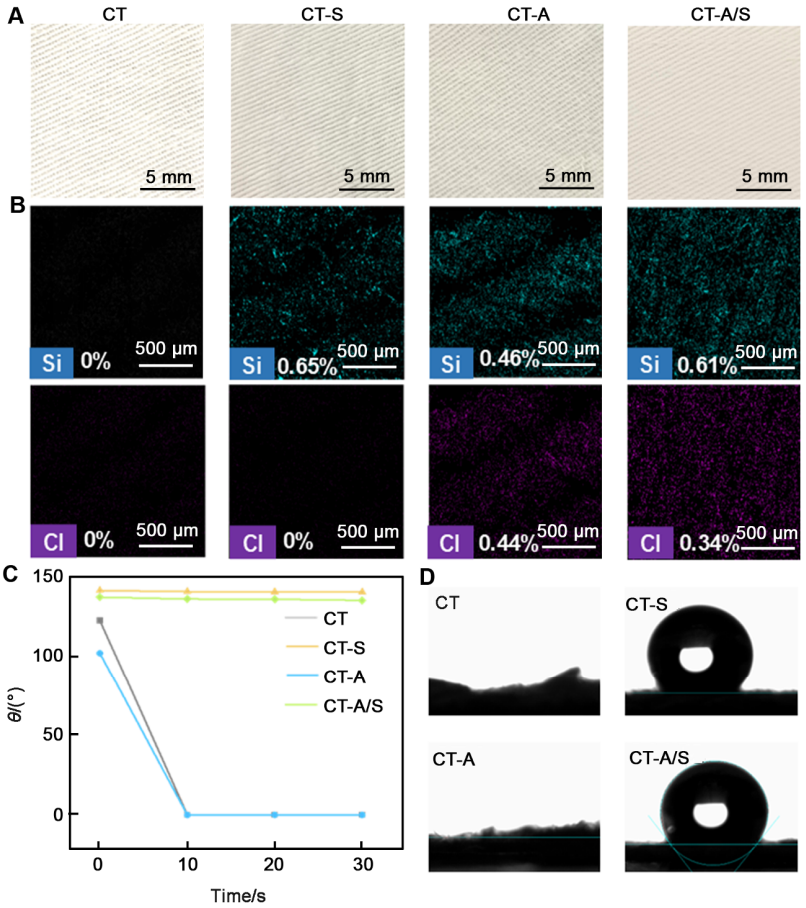


Fig. 1 Characterization of CT, CT-S, CT-A and CT-A/S
(A) Macroscopic view of modified CT; (B) distribution of C and Si in CT after modification observed by EDS; (C) curve of WCA variation; (D) final State Diagram of WCA.

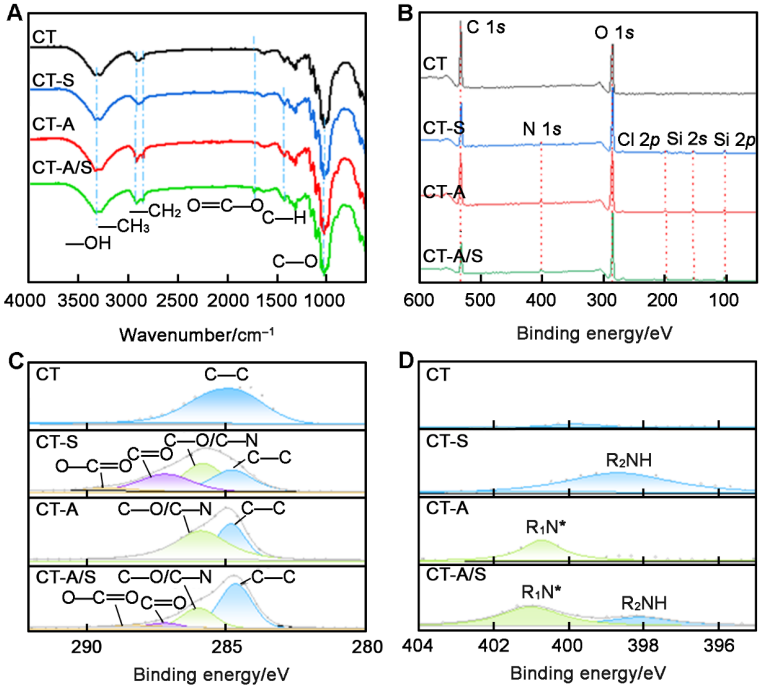


Fig. 2 Material characterization by FTIR and XPS
(A) FTIR spectra of modified CT; (B) XPS wide-scan spectra before and after modification; (C, D) high-resolution XPS spectra of C (C) and N (D).

https://doi.org/10.1007/s40242-026-6123-z

materials were also analyzed using X-ray photoelectron spectroscopy (XPS). The XPS broad-scan spectra of the different samples are shown in Fig. 2B. Compared with CT, the additional N 1*s*, Si 2*s*, and Si 2*p* peaks observed in the spectra can be attributed to the amino and siloxane moieties in SBA and AEM-5700, respectively, while the Cl 2*p* peaks originate from Cl^- in AEM-5700.

As can be seen from the C spectra of the different samples (Fig. 2C), the CT raw material contains only C—C bonds on the cellulose surface; therefore, a single peak appears only at a binding energy of 284.8 eV. The binding energies of C—O/C—N are in the range of 285.5—287.0 eV, those of C═O are in the range of 287.0—289.0 eV, and those of O—C═O are in the range of 288.0—290.0 eV. The CT-S surface was grafted with SBA, resulting in the presence of various bonds, such as C—C, C—O, C—N, C═O, and O—C═O on the surface. The CT-A surface is grafted with 3-(trimethoxysilyl)propyl dimethyl octadecyl ammonium chloride, which contains C—C, C—O, and C—N bonds; the CT-A/S surface includes the aforementioned bonds. It can be observed that CT-S, CT-A, and CT-A/S all exhibit their respective characteristic peaks.

As shown in the N spectra of the different samples (Fig. 2D), only the cellulose surface in the CT raw material is essentially nitrogen-free; however, nitrogen-containing reagents may have been used during processing and preservation, resulting in slight peak fluctuations. The nitrogen of the quaternary amine appears at a binding energy of 398.0—400.0 eV, the nitrogen of QAS appears at a binding energy of 400.5—401.5 eV, and the nitrogen of SBA belongs to secondary amines, so the CT-S material exhibits characteristic peaks at a binding energy of 398.0—400.0 eV; AEM-5700 is a QAS, so the CT-A material exhibits a characteristic peak at a binding energy of 400.5—401.5 eV. Material CT-A/S contains both of these groups, so its spectrum includes both the characteristic peak of the secondary amine and that of the QAS.

2.2 Anti-adhesion and Antifungal Results

Fig. 3A shows the plate count results of the bacterial adhesion test. Compared with CT, there was a significant difference in the number of colonies adhering to the modified samples. CT-S exhibited a 98.43%±0.85% inhibition of *Escherichia coli* (*E. coli*) adhesion, while the inhibition of *Staphylococcus aureus* (*S. aureus*) adhesion reached 100%. No live bacteria were detected on either CT-A or CT-A/S, indicating that both CT-A and CT-A/S possess excellent antimicrobial activity.

Fig. 3B demonstrates that SBA exhibits excellent antifungal properties. Due to the dispersal of *Aspergillus niger* (*A. niger*) spores, some spores adhered to the edges of

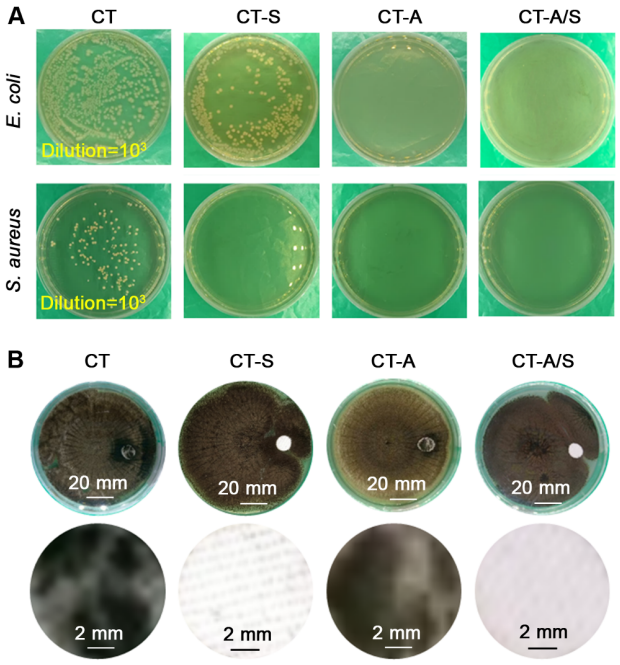


Fig. 3 Antimicrobial properties

(A) Photographs of Tryptic Soy Agar (TSA) plates cultured with eluted *E. coli* and *S. aureus* from various cotton textiles. Labels "Dilution=10^2" denote the serial dilution fold of bacterial suspensions used for viable colony counting; (B) photographs of different fabrics contaminated by *A. niger* after 8 d.

the CT-S material, whereas the antifungal performance of AEM-5700 was less than ideal. CT do not inherently possess antifungal properties, and cotton textiles modified with AEM-5700 also exhibit unsatisfactory antifungal performance, with an antifungal rating of Level 4 (the surface of the material is over 60% covered with fungal contamination); in contrast, cotton textiles modified with SBA achieve excellent results, with an antifungal rating of Level 0 (no obvious fungal contamination on the material surface), indicating that SBA possesses superior antifungal efficacy. At the same time, cotton textiles modified by a blend of the two also achieve excellent antifungal performance, with an antifungal rating of Level 0. In summary, the CT produced by the mixed grafting of the two exhibits ideal antibacterial and antifungal properties.

2.3 Results of the Antimicrobial Model

The antibacterial and wound-healing effects of modified medical gauze were evaluated in a mouse skin wound model of *S. aureus* infection (Fig. 4A). Macroscopic observations of the wounds revealed that, compared with the control group and the standard medical gauze group, the modified gauze group exhibited faster wound healing and more pronounced scab formation and epithelialization (Fig. 4B). Quantitative analysis of wound area further indicated that, over time, wounds in all groups showed a trend toward reduction.

https://doi.org/10.1007/s40242-026-6123-z

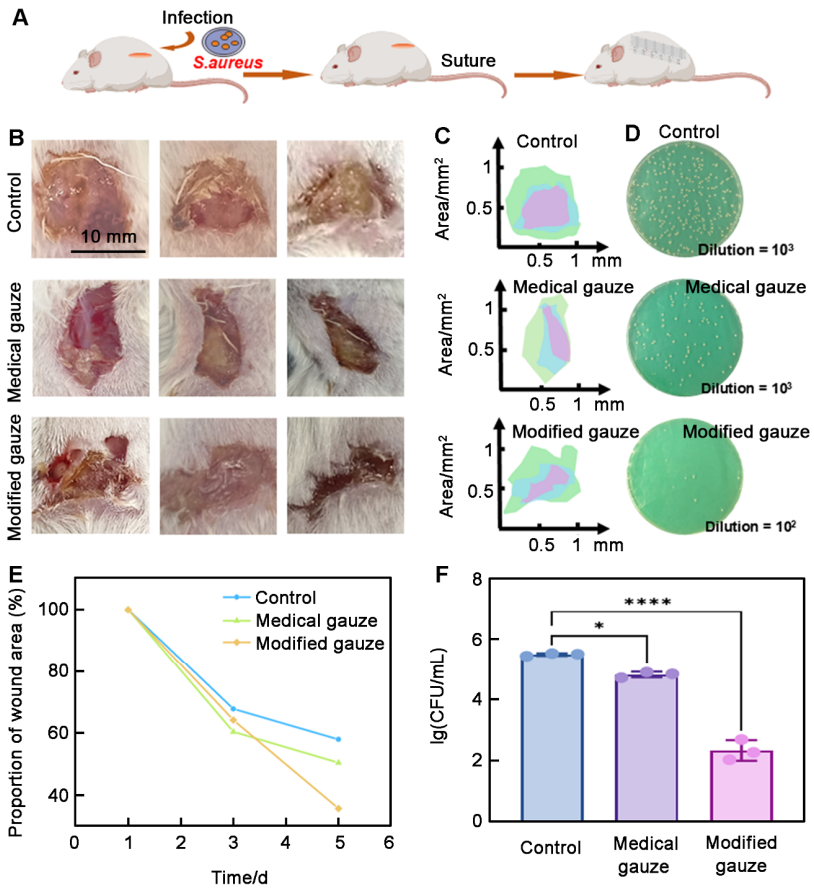


Fig. 4 Experiments on anti-infective models

(A) Antimicrobial model protocol; (B) photos of the rat wound at different time points; (C) changes in wound area; (D) representative TSA plate images of *S. aureus* isolated from wound tissue homogenates. The label "Dilution=10^2" and "Dilution=10^{3}" represent the dilution multiple of wound homogenate prior to spreading; (E) wound area and wound percentage; (F) bacterial counts of the biofilm treated by different groups. Data are expressed as the mean±SD, * p<0.05, ** p<0.01, and **** p<0.0001.

Among them, the rate of wound reduction in the modified gauze group was significantly higher than that in the control group and the standard medical gauze group; by day 5, the proportion of residual wound area was only approximately 35%, far lower than that in the control group (approximately 58%) and the standard medical gauze group (approximately 50%, Fig. 4, C and E).

Analysis of bacterial load in the wound revealed that the control group had the highest *S. aureus* load [lg(CFU/mL)≈4.4]. The standard medical gauze group showed a slight reduction in bacterial load [lg(CFU/mL)≈3.7, p<0.01], whereas the modified gauze group reduced bacterial load to lg(CFU/mL)≈1.9, a difference that was highly significant compared to the control group (p<0.0001), achieving bacterial clearance of approximately two orders of magnitude (Fig. 4, D and F). These results indicate that modified gauze can significantly promote the healing of wounds infected with *S. aureus* by effectively inhibiting bacterial proliferation at the wound site; it has antibacterial and wound-healing effects that are significantly superior to those of conventional medical gauze. The entire animal study was reviewed and approved by the SPF Animal Facility of the Beijing University of Chemical Technology, China (Approval No. BUCT21-2512-078).

3 Conclusions

In summary, we have developed a synergistic antimicrobial strategy that co-immobilizes an organosilicon QAS (AEM-5700) and an organosilicon borneol ester (SBA) onto CT surfaces *via* siloxane hydrolysis and thermal curing. The resulting covalently grafted coating (CT-A/S) integrates the passive defense (anti-adhesion) conferred by the borneol stereochemical motif with the active attack (contact bactericidal action) of the long-chain QAS, thereby endowing CT with exceptional broad-spectrum antimicrobial efficacy against both bacteria and mold, with antimicrobial rates approaching 100%. The covalent anchoring strategy ensures outstanding laundering durability, overcoming the leaching limitations inherent in conventional physical adsorption or pad-dry-cure finishing methods. Furthermore, the *in vivo* mouse infection model validated the potent antibacterial and anti-infective efficacy of the modified textiles, substantiating their clinical translational potential.

This dual-mechanism approach not only addresses the deficiency of QAS-modified textiles in mold resistance and antifouling functionality but also compensates for the limited contact bactericidal capability of borneol ester-based materials when used in isolation. The versatility of the covalent co-grafting methodology renders it readily adaptable to a diverse array of cotton-based healthcare textiles, including surgical gauze, wound dressings, and patient apparel, thereby offering a robust and generalizable platform for infection control in clinical settings. Looking ahead, this strategy is anticipated to inspire the rational design of next-generation antimicrobial surfaces that transcend the traditional trade-off between efficacy and durability, ultimately contributing to the reduction of hospital-acquired infections and the advancement of hygienic healthcare environments.

Supporting Information

The detailed experimental procedures and the supplementary materials are available in the online version of this article at http://dx.doi.org/10.1007/s40242-026-6123-z.

Acknowledgements

This work was supported by the National Science and Technology Major Project, China (No. 2025ZD01902201).

Conflicts of Interest

The authors declare no conflicts of interest.

References

[1] Rather M. A., Gupta K., Bardhan P., Borah M., Sarkar A., Eldiehy K. S. H., Bhuyan S., Mandal M., *J. Basic Microbiol.*, **2021**, *61*, 380.
[2] Morais D., Guedes R., Lopes M., *Materials*, **2016**, *9*, 498.
[3] Zheng S., Liu Y., Yang Y., Zhu R., Yu X., Cao Z., *ACS Appl. Mater. Interfaces*, **2025**, *17*, 46583.
[4] Spagnolo A. M., *Pathogens*, **2024**, *13*, 181.
[5] Laxminarayan R., Matsoso P., Pant S., Brower C., Røttingen J.-A., Klugman K., Davies S., *Lancet*, **2016**, *387*, 168.
[6] Högberg L. D., Heddini A., Cars O., *Trends Pharmacol. Sci.*, **2010**, *31*, 509.
[7] Nadagouda M. N., Vijayasarathy P., Sin A., Nam H., Khan S., Parambath J. B. M., Mohamed A. A., Han C., *Med. Chem. Res.*, **2022**, *31*, 1663.
[8] Wang S., Qiu B., Shi J., Wang M., *J. Coat. Technol. Res.*, **2024**, *21*, 87.
[9] Liao L., Ke Z., Li S., Wang S., Wang X., Rao X., *Chem. Eng. J.*, **2025**, *506*, 159746.
[10] Saseendran Nair S., Anand V., De Silva K., Wiles S., Swift S., *J. Appl. Microbiol.*, **2022,** *133*, 2583.
[11] Feng Y., Zhang D., Liang Y., Yin X., Lei B., *Ind. Crops Prod.*, **2021**, *174*, 114160.
[12] Zhou Y., Jiang Y., Zhang Y., Tan L., *ACS Appl. Mater. Interfaces*, **2022**, *14*, 38358.
[13] Li J., Sha Z., Zhang W., Tao F., Yang P., *J. Biomater. Sci. Polym. Ed.*, **2016**, *27*, 1017.
[14] Xie Z., Chen C., Chen X., Bu F., Li G., Zhang P., Wang X., *React. Funct. Polym.*, **2024**, *202*, 105993.
[15] Cheng Q., Peng Y. Y., Asha A. B., Zhang L., Li J., Shi Z., Cui Z., *Narain R., Biomater. Sci.*, **2022**, *10*, 1787.
[16] Song F., Zhang L., Chen R., Liu Q., Liu J., Yu J., Liu P., Duan J., Wang J., *ACS Appl. Mater. Interfaces*, **2021**, *13*, 33417.
[17] Shi B., Luan D., Wang S., Zhao L., Tao L., Yuan Q., Wang X., *RSC Adv.*, **2015**, *5*, 51947.
[18] Ma R., Lu D., Wang J., Xie Q., Guo J., *Biomed. Pharmacother.*, **2023**, *164*, 114668.
[19] Xin Y., Zhao H., Xu J., Xie Z., Li G., Gan Z., Wang X., *Carbohydr. Polym.*, **2020**, *228*, 115378.
[20] Zhang P., Chen X., Bu F., Chen C., Huang L., Xie Z., Li G., Wang X., *ACS Appl. Mater. Interfaces*, **2023**, *15*, 9926.
[21] Luo L., Li G., Luan D., Yuan Q., Wei Y., Wang X., *ACS Appl. Mater. Interfaces*, **2014**, *6*, 19371.
[22] Xu J., Bai Y., Wan M., Liu Y., Tao L., Wang X., *Polymers*, **2018**, *10*, 448.
[23] Sun X., Xie Y., Ma X., He Y., Song P., Wang R., *Macromolecules*, **2025**, *58*, 4021.